Medicinal Chemistry Research (2024) 33:164–176
https://doi.org/10.1007/s00044-023-03176-x

MEDICINAL CHEMISTRY RESEARCH

ORIGINAL RESEARCH ARTICLE

Indazole derivatives as novel inhibitors of monoamine oxidase and D-amino acid oxidase

Chezélle Stear[1] · Anél Petzer[1,2] · Chantalle Crous[1] · Jacobus P. Petzer[1,2]

Received: 28 September 2023 / Accepted: 26 November 2023 / Published online: 15 December 2023

Abstract

The monoamine oxidase (MAO) enzymes metabolize neurotransmitter amines in the peripheral and central tissues, and inhibitors of these enzymes find application in the treatment of neuropsychiatric and neurodegenerative disorders. Based on reports that the neuronal nitric oxide synthase (nNOS) inhibitor, 7-nitroindazole, inhibits the MAO-B isoform, the present study investigated the MAO inhibition potencies of a synthetic series of fifteen C5- and C6-substituted indazole derivatives. While only one derivative (5c) was a submicromolar inhibitor of human MAO-A ($IC_{50} = 0.745\ \mu M$), all compounds inhibited human MAO-B with submicromolar IC_{50} values. Substitution on C5 of indazole yielded particularly potent MAO-B inhibition with IC_{50} values that ranged from 0.0025–0.024 μM. Further investigation of a selected indazole derivative showed a competitive mode of MAO inhibition. To further explore the pharmacological properties of the indazole derivatives, they were also evaluated as potential inhibitors of porcine D-amino acid oxidase (DAAO). None of the synthetic compounds were noteworthy DAAO inhibitors, however, 1*H*-indazol-5-ol, a synthetic precursor, was found to be a good potency inhibitor with an IC_{50} value of 2.03 μM.

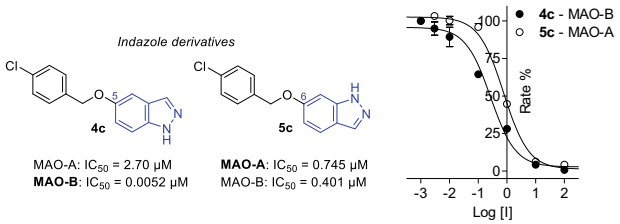

Keywords Monoamine oxidase · MAO · D-amino acid oxidase · DAAO · Inhibitor · Competitive

Introduction

Various neurological disorders have been attributed to dysfunctional neurotransmission and include Parkinson's disease, major depressive disorder and schizophrenia [1–3]. The observation that inhibition of enzymes such as monoamine oxidase (MAO; E.C. 1.4.3.4) and D-amino acid oxidase (DAAO; E.C. 1.4.3.3) increase monoaminergic and glutamatergic function, respectively, has led to an interest in the pharmacological potential of inhibitors of these enzymes in the palliative treatment of neuropsychiatric and neurodegenerative disorders [4, 5].

MAO is a mitochondrial bound flavoenzyme that is widely distributed throughout the body with high expression levels in both peripheral and nervous system tissues [6, 7]. These proteins are the primary degradative enzymes of monoamine neurotransmitters as well as various endogenous and exogenous amines [8]. MAO consists of two isozymes termed MAO-A and MAO-B. Even though these isozymes share 70% amino acid sequence homogeneity, MAO-A and MAO-B exhibit different substrate and

✉ Jacobus P. Petzer
jacques.petzer@nwu.ac.za

[1] Centre of Excellence for Pharmaceutical Sciences, North-West University, Potchefstroom 2520, South Africa

[2] Pharmaceutical Chemistry, School of Pharmacy, North-West University, Potchefstroom 2520, South Africa

inhibitor specificities [9, 10]. MAO-A metabolizes bulkier neurotransmitter amines such as serotonin, whereas MAO-B prefers smaller, non-hydroxylated amines as substrates (e.g., phenethylamine and benzylamine). Certain amines including dopamine, epinephrine and norepinephrine, tyramine and tryptamine are oxidized by both isozymes [5]. Primary amine substrates undergo MAO-catalyzed oxidative deamination to yield the corresponding aldehyde species with ammonia and hydrogen peroxide forming as by-products [11].

MAO regulates neurotransmitter levels and prevents certain extraneous molecules (e.g., dietary amines) from acting as false neurotransmitters, and metabolism facilitated by MAO is thus essential for the correct functioning at synaptic junctions [12]. Overactivity of MAO has been implicated in various psychiatric disorders. Elevated MAO-A density in different brain regions may be responsible for reducing monoamine levels (e.g., serotonin, norepinephrine and dopamine) during major depression and inhibitors of MAO-A have been used for the treatment of depression [13–15]. Similarly, MAO-B expression increases with age in the human brain, and MAO-B inhibitors have been used to treat age-related neurodegenerative disorders such as Parkinson's disease [16, 17]. The rationale behind the use of MAO-B specific inhibitors is that these agents maintain synaptic dopamine levels by preventing its metabolism (or indirectly by elevating phenethylamine levels), thereby alleviating the motor symptoms of Parkinson's disease [18, 19]. When combined with levodopa, MAO-B inhibitors may improve motor fluctuations and allow for a reduction of the levodopa dose [19]. Furthermore, MAO-mediated metabolism is a prominent source of hydrogen peroxide in the central nervous system and this by-product may contribute to neurodegeneration in Parkinson's disease [20]. Under certain conditions, hydrogen peroxide might be converted to hydroxyl free radicals that cause oxidative stress and neuronal damage. This process has been linked with neurodegeneration observed in Parkinson's disease and can potentially form part of the disease pathology [6, 21]. By attenuating hydrogen peroxide production, MAO inhibitors may thus possess neuroprotective effects and MAO-B inhibitors have been advocated as potential disease modifying agents [8, 22–24]. MAO-B inhibitors are a safe and well-tolerated approach in the symptomatic treatment of early or mild Parkinson's disease and although these agents offer only modest symptomatic benefit, they reduce motor fluctuations caused by long-term use of levodopa, slow the rate of clinical decline and improve the efficacy of a lower levodopa dosage [19, 25, 26].

DAAO is a flavoenzyme that metabolizes D-amino acids such as D-alanine and D-serine [27, 28]. DAAO serves a regulatory function in the brain since it metabolizes the endogenous gliotransmitter, D-serine, which acts as a co-agonist that potentiates N-methyl-D-aspartate (NMDA) receptor-mediated neurotransmission by binding to its strychnine-insensitive glycine site [29, 30]. Hypofunction of the NMDA receptor has been implicated in the pathophysiology of schizophrenia, and D-serine and DAAO inhibitors have therefore been investigated for the treatment of schizophrenia [4, 31]. As adjuvant to antipsychotic drugs, D-serine has been shown to reduce the neurocognitive symptoms in schizophrenia [32, 33]. The poor blood-brain barrier permeability of D-serine, however, requires high doses to be administered which may lead to nephrotoxicity [34, 35]. DAAO inhibitors have been investigated as a potential treatment strategy for the positive and negative symptoms associated with schizophrenia. DAAO inhibitors would reduce the central metabolism of D-serine and thus enhance NMDA receptor-mediated neurotransmission [4, 36]. Most synthetic DAAO inhibitors are small molecules that contain the carboxylic acid group or isosteres thereof [31, 37, 38]. Several good potency DAAO inhibitors have been reported as exemplified by 3-hydroxycoumarin (**1**) and 3-hydroxyquinolin-2(1*H*)-one (**2**) (Fig. 1) [27, 31].

In previous studies, the neuronal nitric oxide synthase (nNOS) inhibitor, 7-nitroindazole (**3**), also demonstrated moderate MAO-B inhibition activity ($K_i = 4\,\mu M$) [39, 40]. As with most small molecule inhibitors, 7-nitroindazole is expected to bind to the substrate cavity of the MAO-B enzyme, leaving the entrance cavity unoccupied [41–43]. In general, larger inhibitors that span both cavities are more potent due to the additional interactions formed between the inhibitor and the hydrophobic environment of the entrance cavity [43]. Appropriate substitution with a benzyloxy moiety has been reported to enhance the inhibitory efficacy of similar small molecules by enabling the compound to span both the entrance and substrate cavities of MAO-B [42, 44]. Based on these considerations, a series of C5- and C6-substituted indazole derivatives was synthesized in an attempt to improve the inhibition potency of 7-nitroindazole. The C5 and C6 positions were selected for substitution since literature showed that the MAO-B inhibition potency of another small molecule inhibitor, isatin, was significantly enhanced by substitution at the analogous positions [44, 45]. Substitution at these positions would direct the substituent into the entrance cavity. The series of indazole derivatives was evaluated as potential in vitro inhibitors of MAO-A, MAO-B and DAAO. Although there

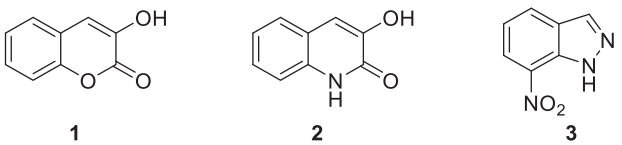

Fig. 1 The structures of 3-hydroxycoumarin (**1**), 3-hydroxyquinolin-2(1*H*)-one (**2**) and 7-nitroindazole (**3**)

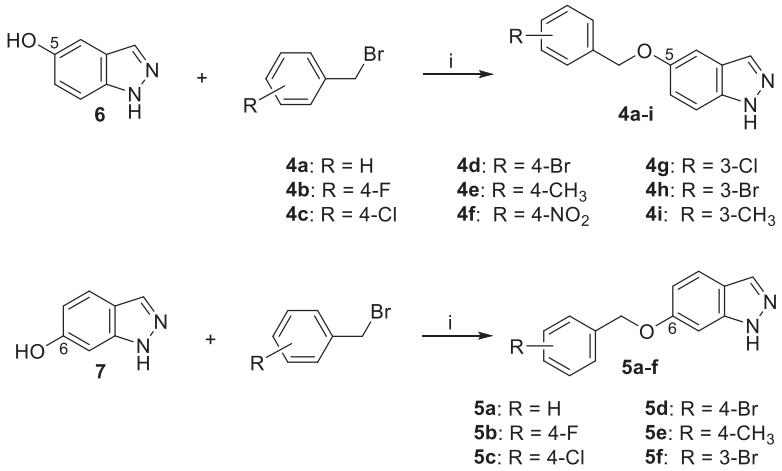

Fig. 2 Synthetic route to C5- and C6-substituted indazoles **4a–i** and **5a–f**. Key: (i) DMF, K_2CO_3, rt, 24 h

is no structural rationale for these compounds to act as DAAO inhibitors, the evaluation was used for comparison with the MAO inhibition potencies and for the generation of selectivity data.

Results and discussion

Chemistry

The indazole derivatives (**4** and **5**) were synthesized according to the method reported in literature. In the presence of K_2CO_3, commercially available 1*H*-indazol-5-ol (**6**) or 1*H*-indazol-6-ol (**7**) was dissolved in DMF and reacted with the appropriate alkyl bromides to produce the desired derivatives (Fig. 2). The yields of the reactions ranged from 3.1 to 22.8% (**4a–i**) and 10.2 to 18.4 (**5a–f**). The products were characterized by NMR and mass spectrometry (see supplementary material).

Monoamine oxidase inhibition

The C5- and C6-substituted indazole derivatives synthesized in this study were evaluated as potential in vitro inhibitors of human MAO-A and MAO-B. The recombinant MAO enzymes were utilized to determine the inhibition properties of the compounds, while kynuramine served as a mixed MAO-A/B substrate. MAO metabolizes kynuramine to yield 4-hydroxyquinoline as final product. The production of 4-hydroxyquinoline was monitored by fluorescence spectrophotometry since the compound fluoresces in an alkaline environment. The enzyme reactions were thus carried out in the presence of a range of inhibitor concentrations (0.003–100 μM). After 20 min have elapsed, the reactions were terminated by the addition of sodium hydroxide and the formation of 4-hydroxyquinoline was quantitated. The enzyme catalytic activities were calculated and sigmoidal graphs of activity versus the logarithm of inhibitor concentration (log[I]) were constructed from triplicate experiments. These graphs were used to estimate IC_{50} values, which are reported in Table 1. Examples of sigmoidal graphs for the estimation of IC_{50} values are presented in Fig. 3.

The results of the inhibition studies showed that most of the indazole derivatives inhibited MAO-A with the most potent inhibition recorded for **5c** ($IC_{50} = 0.745$ μM). This compound was the only submicromolar MAO-A inhibitor of the series. Among the test series, nine compounds exhibited $IC_{50} < 10$ μM and thus possessed potencies that were similar to the reference inhibitors isatin ($IC_{50} = 8.29$ μM) and toloxatone ($IC_{50} = 1.67$ μM). The following structure-activity relationships were noted for the inhibition of MAO-A: (a) The C6-substituted derivatives were more potent than the corresponding C5-substituted homologs (e.g., **4a** vs. **5a**; **4b** vs. **5b**; **4c** vs. **5c**; **4d** vs. **5d**; **4h** vs. **5f**). (b) For both the C5- and C6-substituted derivatives, the 4-chloro substituted compounds (**4c** and **5c**) were the most potent MAO-A inhibitors while the methyl substituted compounds (**4e, 4i, 5e**) did not inhibit MAO-A at a maximal tested concentration of 100 μM. (c) It was interesting to note that neither 1*H*-indazol-5-ol (**6**) nor 1*H*-indazol-6-ol (**7**) inhibited MAO-A which demonstrated the requirement of a C5 or C6 substituent for inhibition.

The indazole derivatives were significantly more potent inhibitors of MAO-B compared to the MAO-A isoform, with all derivatives exhibiting $IC_{50} < 1$ μM. Based on their potency ranges, it was clear that the C5-substituted derivatives were more potent MAO-B inhibitors compared to the C6-substituted derivatives. For the C6-substituted derivatives, the IC_{50} values ranged from 0.118–0.979 μM while those of the C5-substituted derivatives ranged from 0.0025–0.024 μM, a difference of one to two orders of magnitude. The C5-substituted derivatives were therefore significantly more potent than the reference inhibitor

Table 1 The potencies (IC_{50} values) of the inhibition of human MAO-A and MAO-B, and porcine DAAO by the indazole derivatives (**4a–i, 5a–f**) and reference inhibitors

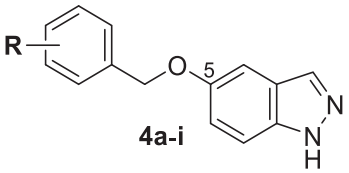

4a-i

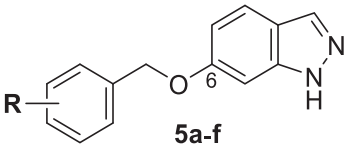

5a-f

	R	IC_{50} (μM)[a]		
		MAO-A	MAO-B	DAAO
4a	H	NI[b]	0.024 ± 0.010	NI[b]
4b	4-F	7.65 ± 0.310	0.0051 ± 0.0003	NI[b]
4c	4-Cl	2.70 ± 0.527	0.0052 ± 0.0008	107 ± 3.70
4d	4-Br	NI[b]	**0.0025 ± 0.0012**	80.5 ± 7.92
4e	4-CH_3	NI[b]	0.0042 ± 0.0003	NI[b]
4f	4-NO_2	3.85 ± 0.179	0.0052 ± 0.0006	91.6 ± 37.1
4g	3-Cl	7.42 ± 0.625	0.0031 ± 0.0009	102 ± 22.9
4h	3-Br	6.39 ± 0.417	0.0035 ± 0.0002	60.5 ± 27.8
4i	3-CH_3	NI[b]	0.012 ± 0.004	NI[b]
5a	H	17.2 ± 1.48	0.979 ± 0.103	NI[b]
5b	4-F	3.28 ± 0.227	0.247 ± 0.062	NI[b]
5c	4-Cl	**0.745 ± 0.060**	0.401 ± 0.027	NI[b]
5d	4-Br	1.20 ± 0.039	0.565 ± 0.031	NI[b]
5e	4-CH_3	NI[b]	0.491 ± 0.034	NI[b]
5f	3-Br	2.51 ± 0.067	0.118 ± 0.012	NI[b]
Isatin[c]		8.29 ± 1.25	5.99 ± 2.92	–
1*H*-Indazol-5-ol (**6**)		NI[b]	NI[b]	**2.03 ± 0.188**
1*H*-Indazol-6-ol (**7**)		NI[b]	NI[b]	NI[b]
Toloxatone[c]		1.67 ± 0.418	–	NI[b]
Safinamide[c]		–	0.240 ± 0.080	–
3-Methylpyrazole-5-carboxylic acid[c]		–	–	2.04 ± 0.367

[a]Values are reported as the mean ± standard deviation (SD) of triplicate determinations

[b]NI, no inhibition observed at a maximum concentration of 100 μM

[c]Reference inhibitors

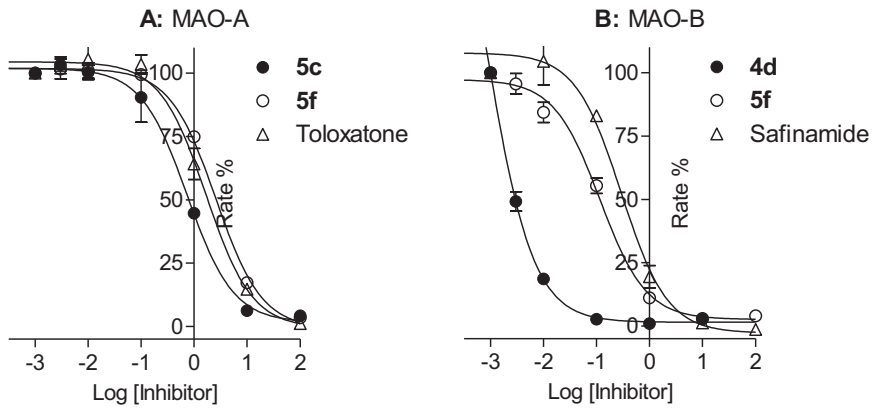

Fig. 3 **A** Sigmoidal graphs for the inhibition of MAO-A by **5c** (filled circles), **5f** (open circles) and toloxatone (triangles). **B** Sigmoidal graphs for the inhibition of MAO-B by **4d** (filled circles), **5f** (open circles) and safinamide (triangles)

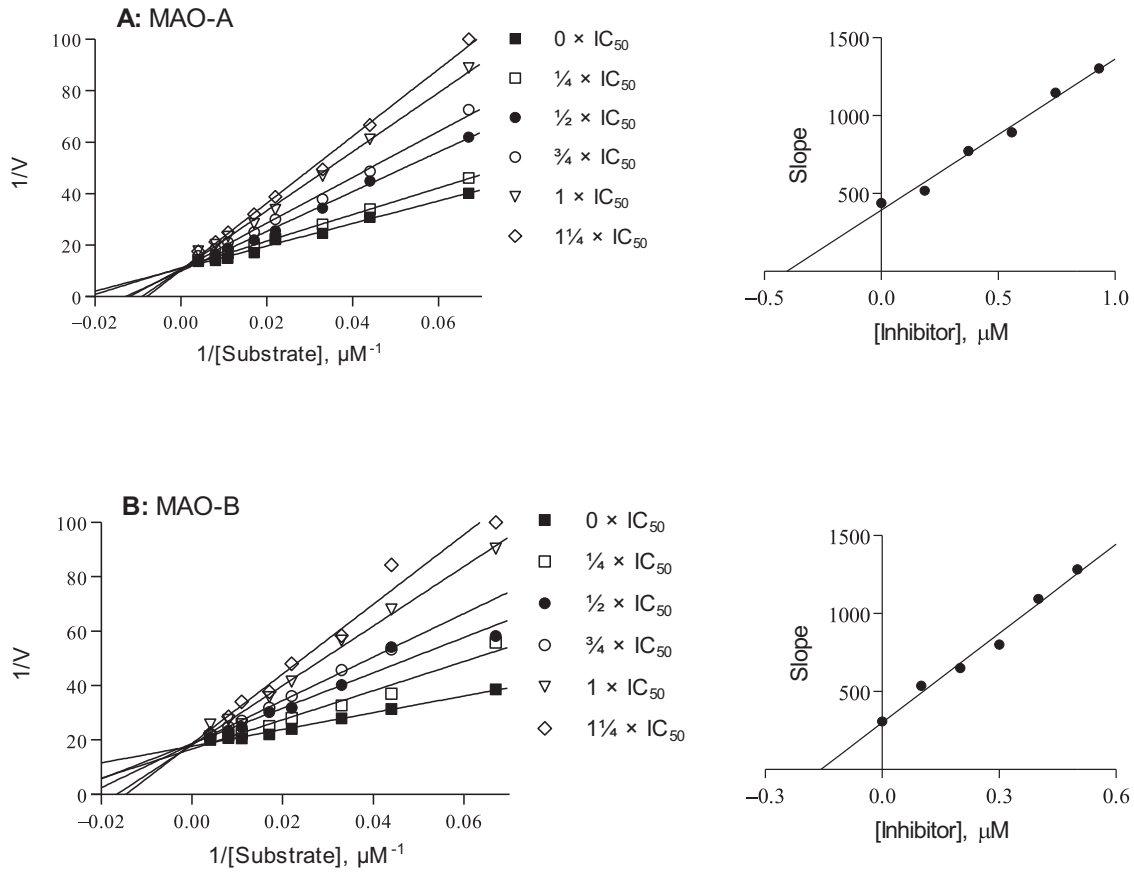

Fig. 4 Lineweaver-Burk graphs for the inhibition of MAO-A (**A**) and MAO-B (**B**) by **5c**. The insets are replots of the slopes of the Lineweaver-Burk plots versus inhibitor concentration, from which K_i values were estimated. For MAO-A the inhibitor concentration ranged from 0.186 to 0.931 μM, while for MAO-B, the inhibitor concentration ranged from 0.1 to 0.5 μM

safinamide ($IC_{50} = 0.240$ μM). The following structure-activity relationships were noted for the inhibition of MAO-B: (a) Among the C5-substituted derivatives, the benzyloxy substituted compound **4a** ($IC_{50} = 0.024$ μM) was the weakest MAO-B inhibitor, which indicated that a substituent (F, Cl, Br, CH_3, NO_2) on the benzyloxy ring enhanced MAO-B inhibition. (b) For the C5-substituted derivatives, substitution on both the C4 and C3 positions of the benzyloxy ring (e.g., **4c** vs. **4g**; **4d** vs. **4h**; **4e** vs. **4i**) resulted in high potency inhibition, while for the C6-substituted derivatives (**5a–f**) substitution on C3 of the benzyloxy ring (**5f**) yielded the most potent inhibitor. In fact, **5f** ($IC_{50} = 0.118$ μM) was approximately fivefold more potent than the C4-substituted homolog **5d** ($IC_{50} = 0.565$ μM). (c) As for MAO-A, neither 1*H*-indazol-5-ol (**6**) nor 1*H*-indazol-6-ol (**7**) inhibited MAO-B which demonstrated the requirement of a C5 or C6 substituent for inhibition.

Since 7-nitroindazole is a reversible competitive inhibitor of MAO-B, it is likely that the indazole derivatives would also act as competitive inhibitors of the MAO enzymes. To further investigate the inhibition properties of the indazole derivative, sets of Lineweaver-Burk graphs were constructed for the inhibition of MAO-A and MAO-B by **5c**. This compound represents a potent inhibitor of the respective MAO isoforms. To construct the Lineweaver-Burk graphs, MAO activities were measured in the absence and presence of the following set of inhibitor concentrations: ¼ × IC_{50}, ½ × IC_{50}, ¾ × IC_{50}, 1 × IC_{50} and 1¼ × IC_{50}. Each Lineweaver-Burk graph was prepared with substrate concentrations ranging from 15 to 250 μM. As shown in Fig. 4, the lines of the Lineweaver-Burk graphs intersected on the y-axis for both MAO-A and MAO-B, which was indicative of competitive inhibition. Replots of the slopes of the Lineweaver-Burk graphs versus inhibitor concentration also yielded linear lines from which the enzyme-inhibitor dissociation constants, K_i, were estimated ($-K_i$ = x-axis intercept). K_i values of 0.40 and 0.16 μM were estimated for the inhibition of MAO-A and MAO-B, respectively, by **5c**.

Molecular docking

A molecular docking study was undertaken to investigate the potential binding modes and interactions of selected

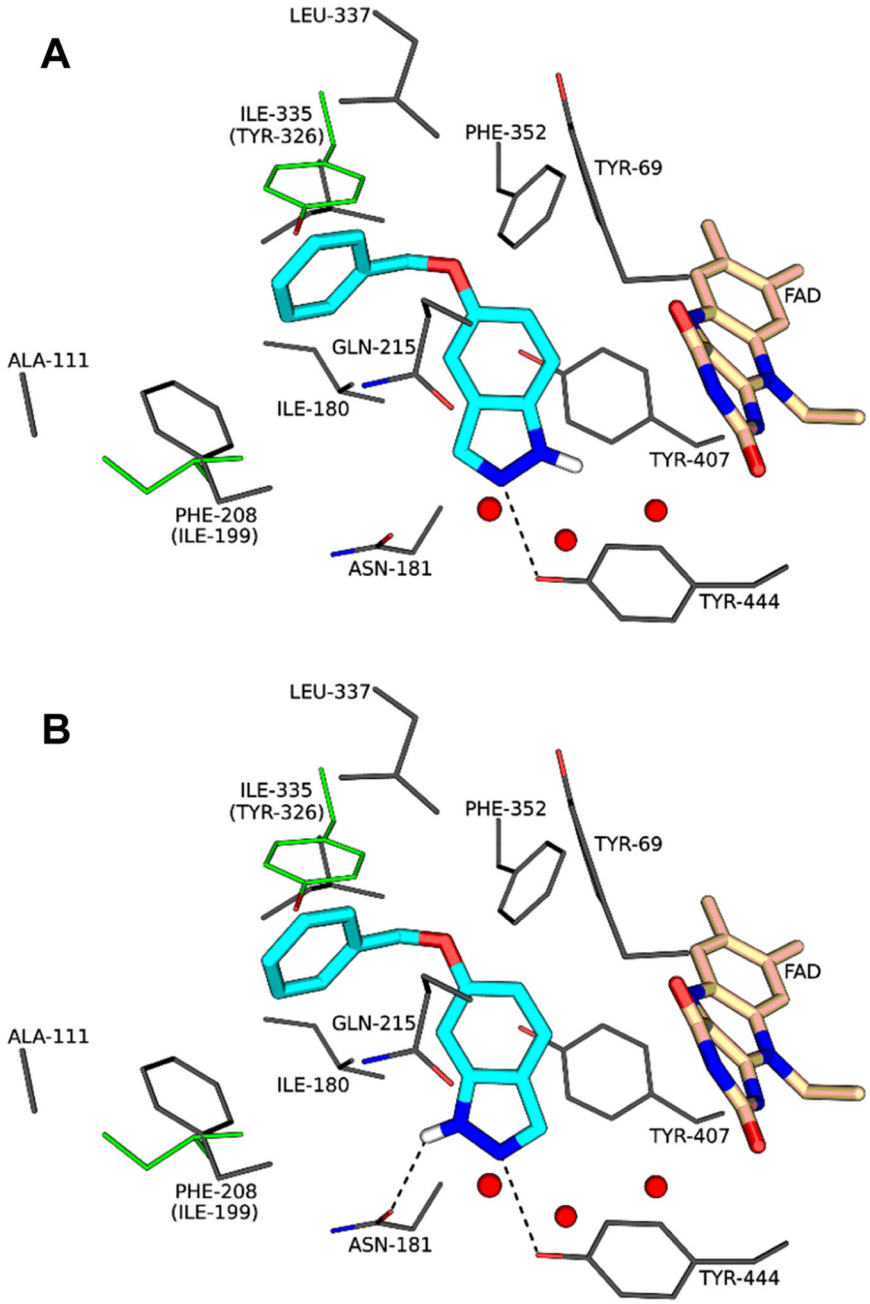

Fig. 5 The predicted binding of **4a** (**A**) and **5a** (**B**) to the active site of human MAO-A. Hydrogen bonding is indicated by dashed lines. Residues Ile-199 and Tyr-326 in MAO-B, which correspond to Phe-208 and Ile-335 in MAO-A, respectively, are shown in green with the labels bracketed

indazole derivatives (**4a** and **5a**) in the active sites of MAO-A and MAO-B. For the docking study, the crystal structures of human MAO-A and MAO-B bound to harmine and safinamide, respectively, were used [42, 46]. The CDOCKER module of the Discovery Studio 3.1 suite of software was used and the protocol reported in literature was followed [47]. The predicted binding modes of **4a** and **5a** to MAO-A are presented in Fig. 5 and show that the inhibitors adopted virtually identical orientations in the active site, with the only difference being that the indazole ring is rotated through 180 ° between the two derivatives. As a result, **5a** formed a hydrogen bond interaction with Asn-181 in addition to that observed with Tyr-444 for both derivatives. Other stabilizing interactions included pi interactions of the benzyloxy ring of the inhibitors with Phe-208 and both indazole rings with Tyr-407.

The predicted binding modes of **4a** and **5a** to MAO-B are presented in Fig. 6. As for MAO-A, the inhibitors adopted similar binding orientations with the only difference being that the indazole ring was rotated through 180 °. A hydrogen bond interaction was observed between the inhibitors and Tyr-435. The MAO-B active site consists of two cavities, an entrance cavity which leads to a substrate cavity. For the inhibitors, the indazole ring was located in

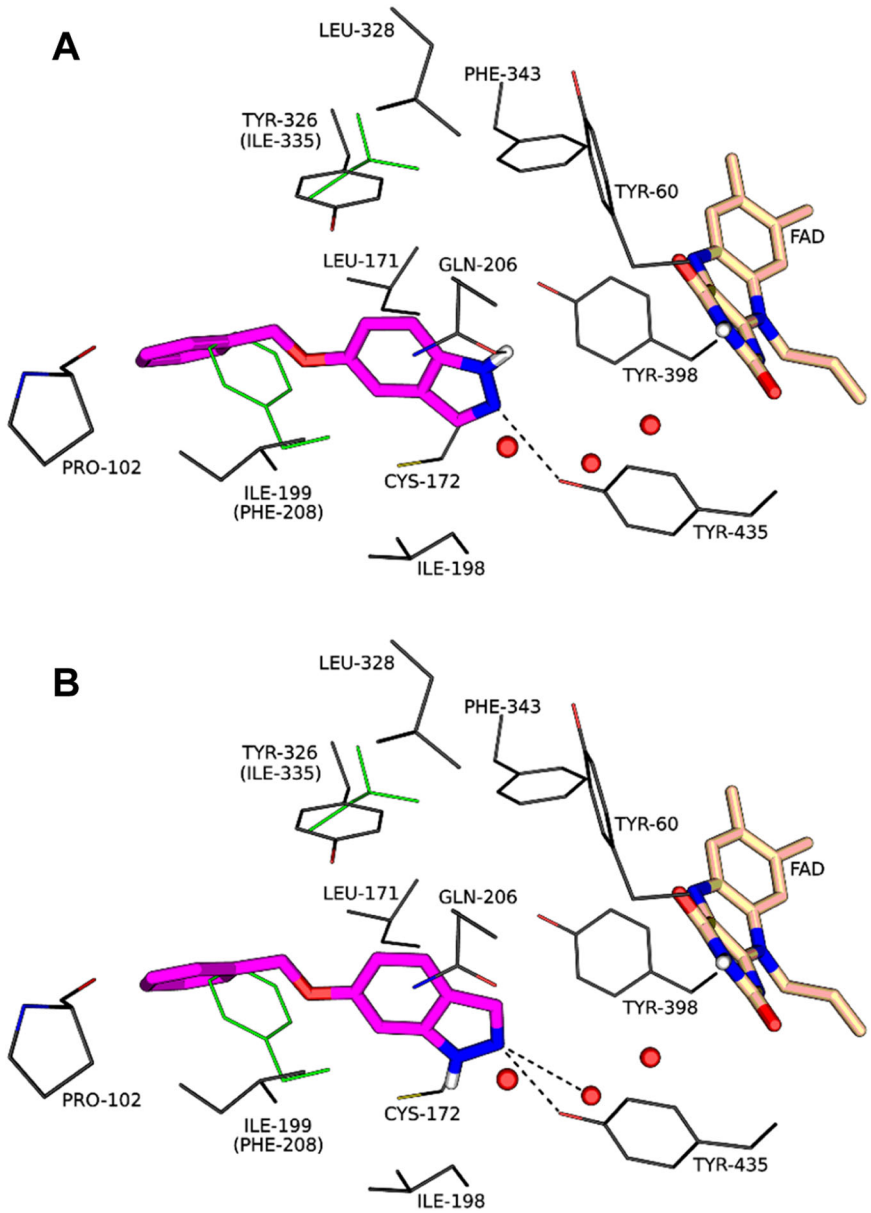

Fig. 6 The predicted binding of **4a** (**A**) and **5a** (**B**) to the active site of human MAO-B. Hydrogen bonding is indicated by dashed lines. Residues Phe-208 and Ile-335 in MAO-A, which correspond to Ile-199 and Tyr-326 in MAO-B, respectively, are shown in green with the labels bracketed

the substrate cavity while the benzyloxy ring extended into the entrance cavity. These compounds were thus cavity spanning inhibitors of MAO-B. Such compounds are reported to possess higher affinity for MAO-B due to the additional interactions provided by the entrance cavity compared to compounds that bind only to the substrate cavity [43]. Other interactions between the derivatives and MAO-B included a pi interaction between the phenyl of the indazole ring system and Tyr-326 and a pi-sulfur interaction between both rings of the indazole and Cys-172.

D-Amino acid oxidase inhibition

DAAO from porcine kidney was used to investigate the inhibition properties of the indazole derivatives, while D-serine served as the substrate. The catalytic activity of DAAO was determined by measuring the production of H_2O_2 via continuous fluorescence spectrophotometry [37, 48]. The formation of H_2O_2 was measured in a peroxidase-coupled assay, where Amplex red is oxidized to produce the fluorescent compound, resorufin. DAAO and D-serine were incubated in the presence of various inhibitor concentrations (0.003–100 µM) while the fluorescence intensities were continuously monitored. Sigmoidal graphs of the rate of change in fluorescence vs. inhibitor concentration (log [I]) were constructed from triplicate experiments, and the IC_{50} values were calculated using these plots. The IC_{50} values are reported in Table 1 while Fig. 7 presents examples of sigmoidal graphs for the estimation of IC_{50} values.

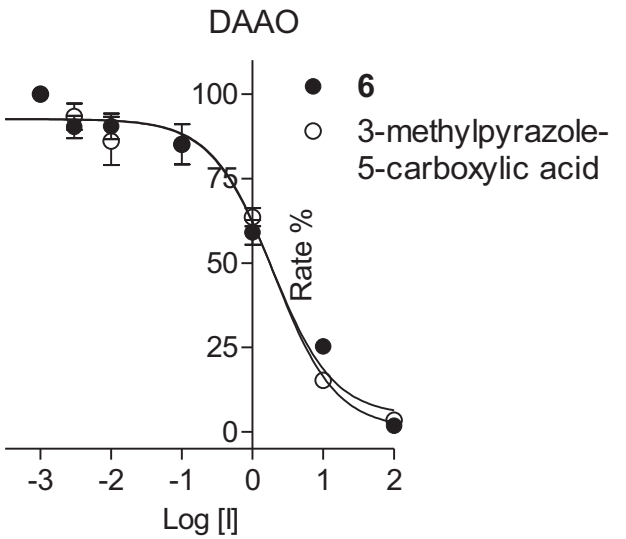

Fig. 7 Sigmoidal graphs for the inhibition of DAAO by 1*H*-indazol-5-ol (**6**) (filled circles) and 3-methylpyrazole-5-carboxylic acid (open circles)

Table 2 Percentage of the fluorescence signal generated from H_2O_2 by the peroxidase-coupled spectrofluorometric assay system in the presence of a test inhibitor (1, 10 and 100 µM) compared to the signal generated in the absence of inhibitor (100%)

	Fluorescence signal (%)[a]		
	1 µM	10 µM	100 µM
1*H*-Indazol-5-ol (**6**)	96 ± 4.1	92 ± 4.6	24 ± 1.1
3-Methylpyrazole-5-carboxylic acid[b]	93 ± 1.1	89 ± 1.0	86 ± 2.5

[a]Values are reported as the mean ± SD of triplicate determinations

[b]Reference inhibitor

The results showed that only five of the indazole derivatives exhibited weak DAAO inhibition with the most potent inhibition recorded for **4h** ($IC_{50} = 60.5$ µM). Interestingly, all five of the compounds that showed inhibition were C5-substituted indazoles. However, 1*H*-indazol-5-ol (**6**) was found to be a good potency inhibitor with an IC_{50} value of 2.03 µM, whereas 1*H*-indazol-6-ol (**7**) did not inhibit the enzyme. The inhibition potency of **6** was thus similar to that of the reference inhibitor 3-methylpyrazole-5-carboxylic acid ($IC_{50} = 2.04$ µM).

There existed the possibility that a test compound may suppress the fluorescent signal produced by the peroxidase-coupled spectrofluorometric assay system, which may be incorrectly interpreted as DAAO inhibition. To investigate if this may have occurred for 1*H*-indazol-5-ol (**6**), the effect of the inhibitor on the fluorescence signal generated from hydrogen peroxide was measured. As shown in in Table 2, compound **6** decreased the fluorescent signal slightly at concentrations of 1 and 10 µM (92–96% residual signal), while significant suppression of the signal was observed at 100 µM (24% residual signal). Since the IC_{50} value for the inhibition of DAAO was well below 10 µM, it may be concluded that this compound was a true inhibitor and did not merely interfere with the assay system. For 3-methylpyrazole-5-carboxylic acid, only slight suppression of the fluorescence signal was observed at all tested concentrations.

The observation of the weak inhibition potencies of these compounds is consistent with reports that the binding site of DAAO prefers small and highly polar ligands [49]. Most of the known, good potency DAAO inhibitors are mono- or bicyclic compounds that consist of an acidic functionality (or isostere thereof) without large substituents or side-chains as exemplified by 3-hydroxycoumarin (**1**) and 3-hydroxyquinolin-2(1*H*)-one (**2**) [27, 31]. Despite the fact that the C5- and C6-substituted indazole derivatives are bicyclic, the bulky side-chains most likely prevented the compounds from binding and inhibiting DAAO.

Conclusion

It has been reported that 7-nitroindazole is a moderate MAO-B inhibitor. Since the inhibitory potencies of small molecule compounds can be enhanced with the addition of appropriate substituents, the present study synthesized and evaluated a series of C5 and C6-substituted indazole derivatives as in vitro inhibitors of MAO-A and MAO-B. The most potent inhibitors presented with IC_{50} values of 0.745 µM (**5c**) and 0.0025 µM (**4d**) for MAO-A and MAO-B, respectively. These compounds were more potent inhibitors than the MAO-A and MAO-B reference inhibitors, toloxatone ($IC_{50} = 1.67$ µM) and safinamide ($IC_{50} = 0.240$ µM), respectively. The results documented that the indazole derivatives were more potent MAO-B inhibitors than MAO-A inhibitors. Furthermore, the C5-substituted compounds displayed higher MAO-B inhibition potencies than the corresponding C6-substituted analogs. It may be concluded that the MAO-B inhibitors identified in this study could serve as lead compounds for the development of drugs for the treatment of Parkinson's disease. However, none of the indazole derivatives exhibited good potency inhibition of DAAO. This might be attributed to the bulky side-chains resulting from substitution with the benzyloxy moiety that hindered the analogs from binding to the DAAO enzyme.

Experimental

Materials and instrumentation

Chemical reagents

The solvents and reagents used for the synthetic procedures were obtained from Sigma-Aldrich. Deuterated

dimethylsulfoxide (DMSO-d_6) used for nuclear magnetic resonance (NMR) spectroscopy was procured from Merck.

NMR

A Bruker Avance III 600 spectrometer was used to record proton (^{1}H) and carbon (^{13}C) NMR spectra at frequencies of 600 MHz and 150 MHz, respectively. The integration, multiplicity, and coupling constants (J), which are given in hertz (Hz), are included in the notation of the spectra. Chemical shifts (δ) are reported in parts per million (ppm) and were referenced to the residual solvent (DMSO-d_6) signal at 2.5 ppm for ^{1}H NMR and 39.5 ppm for ^{13}C NMR. Spin multiplicities are denoted as s (singlet), d (doublet), dd (doublet of doublets), t (triplet) or m (multiplet).

Mass spectrometry

High resolution mass spectra (HRMS) were obtained with a Bruker micrOTOF-Q II mass spectrometer using atmospheric-pressure chemical ionization (APCI) in the positive mode.

TLC (thin layer chromatography)

The progression and completion of the chemical reactions were monitored by TLC. Silica gel 60 aluminum coated TLC sheets (containing UV254 fluorescent indicator) were used with a mobile phase consisting of ethyl acetate and hexane (3:2).

Biology

Enzymes, substrates and reference inhibitors used for the biological experiments were obtained from Sigma-Aldrich. A Varian Cary Eclipse fluorescence spectrophotometer (Agilent Technologies) and a SpectraMax iD3 multi-mode microplate reader (Molecular Devices) were used to record fluorescence measurements of all enzymatic reactions.

The synthesis of C5- (4a–i) and C6-substituted (5a–f) indazoles

1*H*-Indazol-5-ol or 1*H*-indazol-6-ol (4 mmol) was dissolved in anhydrous N,N-dimethylformamide (DMF, 10 mL) at room temperature, after which potassium carbonate (K_2CO_3, 8 mmol) was added. The appropriate alkyl bromide (5 mmol for **4a–f** and **5a–f**, 4.5 mmol for **4g–i**) was subsequently added and the reaction was stirred at 0 °C for 2 h. The reaction was allowed to warm to room temperature and stirring was continued for 24 h. Upon completion, water (50 mL) was added and the resulting precipitate was collected by filtration and dried under vacuum. Compounds **5a–c** were purified by recrystallisation from ethanol. Silica gel column chromatography (ethyl acetate:hexane, 4:1) was used to purify compounds **5d–f** and **4a–i**.

5-(Benzyloxy)-1H-indazole (4a)

Yield: 10.0%; mp 175–177.4 °C; ^{1}H NMR (600 MHz, DMSO-d_6) δ 12.94 (s, 1H), 7.95 (s, 1H), 7.50 – 7.44 (m, 3H), 7.43 – 7.37 (m, 2H), 7.36–7.31 (m, 1H), 7.29 – 7.24 (m, 1H), 7.08 (dd, $J = 9.0$, 2.3 Hz, 1H), 5.12 (s, 2H); ^{13}C NMR (150 MHz, DMSO-d_6) δ 153.24, 137.77, 136.25, 133.29, 128.86, 128.20, 128.14, 123.51, 118.82, 111.53, 101.78, 70.09; APCI-HRMS *m/z*: calculated for $C_{14}H_{13}N_2O$ (MH^+), 225.1022, found 225.1018.

5-[(4-Fluorophenyl)methoxy]-1H-indazole (4b)

Yield: 22.8%; mp 177.7-179.5 °C; ^{1}H NMR (600 MHz, DMSO-d_6) δ 12.91 (s, 1H), 7.95 (s, 1H), 7.56 – 7.50 (m, 2H), 7.46 (d, $J = 8.9$ Hz, 1H), 7.29 – 7.25 (m, 1H), 7.25 – 7.19 (m, 2H), 7.08 (dd, $J = 8.9$, 2.3 Hz, 1H), 5.10 (s, 2H); ^{13}C NMR (150 MHz, DMSO-d_6) δ 162.98, 161.37, 153.15, 136.32, 134.02, 134.00, 133.30, 130.36, 130.31, 123.51, 118.80, 115.72, 115.58, 111.52, 101.97, 69.47; APCI-HRMS m/z: calculated for $C_{14}H_{12}FN_2O$ (MH^+), 243.0928, found 243.0924.

5-[(4-Chlorophenyl)methoxy]-1H-indazole (4c)

Yield: 19.0%; mp 179-181 °C; ^{1}H NMR (600 MHz, DMSO-d_6) δ 12.91 (s, 1H), 7.94 (s, 1H), 7.51 (d, $J = 8.4$ Hz, 2H), 7.48 – 7.44 (m, 3H), 7.30 – 7.22 (m, 1H), 7.08 (dd, $J = 8.9$, 2.3 Hz, 1H), 5.13 (s, 2H); ^{13}C NMR (150 MHz, DMSO-d_6) δ 153.05, 136.87, 136.34, 133.31, 132.75, 129.90, 128.85, 123.50, 118.76, 111.55, 102.03, 69.34; APCI-HRMS m/z: calculated for $C_{14}H_{12}ClN_2O$ (MH^+), 259.0633, found 259.0626.

5-[(4-Bromophenyl)methoxy]-1H-indazole (4d)

Yield: 13.9%; mp 184–187 °C; ^{1}H NMR (600 MHz, DMSO-d_6) δ 12.90 (s, 1H), 7.94 (s, 1H), 7.63 – 7.57 (m, 2H), 7.50 – 7.40 (m, 3H), 7.29 – 7.23 (m, 1H), 7.08 (dd, $J = 8.9$, 2.3 Hz, 1H), 5.11 (s, 2H); ^{13}C NMR (150 MHz, DMSO-d_6) δ 153.04, 137.30, 136.33, 133.31, 131.78, 130.20, 123.50, 121.26, 118.75, 111.55, 102.05, 69.37; APCI-HRMS m/z: calculated for $C_{14}H_{12}BrN_2O$ (MH^+), 303.0128, found 303.0142.

5-[(4-Methylphenyl)methoxy]-1H-indazole (4e)

Yield: 15.2%; mp 187-189.9 °C; ^{1}H NMR (600 MHz, DMSO-d_6) δ 12.91 (s, 1H), 7.94 (s, 1H), 7.45 (d, $J = 8.9$ Hz, 1H), 7.36 (d, $J = 7.9$ Hz, 2H), 7.28 – 7.22 (m, 1H), 7.20 (d, $J = 7.8$ Hz, 2H), 7.06 (dd, $J = 8.9$, 2.3 Hz,

1H), 5.06 (s, 2H), 2.31 (s, 3H); ^{13}C NMR (150 MHz, DMSO-d_6) δ 153.26, 137.40, 136.24, 134.73, 133.28, 129.40, 128.22, 123.52, 118.84, 111.48, 101.83, 70.03, 21.23; APCI-HRMS m/z: calculated for $C_{15}H_{15}N_2O$ (MH^+), 239.1179, found 239.1168.

5-[(4-Nitrophenyl)methoxy]-1H-indazole (4f)

Yield: 5.8%; mp 191–193 °C; ^{1}H NMR (600 MHz, DMSO-d_6) δ 12.95 (s, 1H), 8.27 (d, $J = 8.8$ Hz, 2H), 7.95 (s, 1H), 7.76 (d, $J = 8.7$ Hz, 2H), 7.48 (d, $J = 9.0$ Hz, 1H), 7.30 – 7.24 (m, 1H), 7.13 (dd, $J = 9.0$, 2.3 Hz, 1H), 5.31 (s, 2H); ^{13}C NMR (150 MHz, DMSO-d_6) δ 152.81, 147.41, 145.81, 136.39, 133.34, 128.65, 124.05, 123.45, 118.68, 111.67, 102.09, 68.97; APCI-HRMS m/z: calculated for $C_{14}H_{12}N_3O_3$ (MH^+), 270.0873, found 270.0863.

5-[(3-Chlorophenyl)methoxy]-1H-indazole (4g)

Yield: 3.1%; mp 163.5–165 °C; ^{1}H NMR (600 MHz, DMSO-d_6) δ 12.93 (s, 1H), 7.95 (s, 1H), 7.56 – 7.53 (m, 1H), 7.47 (d, $J = 9.0$ Hz, 1H), 7.45 – 7.41 (m, 2H), 7.41–7.38 (m, 1H), 7.29 – 7.23 (m, 1H), 7.10 (dd, $J = 9.0$, 2.3 Hz, 1H), 5.15 (s, 2H); ^{13}C NMR (150 MHz, DMSO-d_6) δ 152.98, 140.42, 136.33, 133.55, 133.32, 130.80, 128.10, 127.70, 126.59, 123.47, 118.75, 111.59, 101.96, 69.20; APCI-HRMS m/z: calculated for $C_{14}H_{12}ClN_2O$ (MH^+), 259.0633, found 259.0637.

5-[(3-Bromophenyl)methoxy]-1H-indazole (4h)

Yield: 7.0%; mp 165–167 °C; ^{1}H NMR (600 MHz, DMSO-d_6) δ 12.91 (s, 1H), 7.95 (s, 1H), 7.70 – 7.66 (m, 1H), 7.53 (d, $J = 8.2$ Hz, 1H), 7.51 – 7.44 (m, 2H), 7.37 (t, $J = 7.8$ Hz, 1H), 7.29 – 7.24 (m, 1H), 7.10 (dd, $J = 9.0$, 2.3 Hz, 1H), 5.14 (s, 2H); ^{13}C NMR (150 MHz, DMSO-d_6) δ 153.00, 140.69, 136.36, 133.33, 131.08, 131.00, 130.57, 126.98, 123.49, 122.14, 118.74, 111.58, 102.03, 69.20; APCI-HRMS m/z: calculated for $C_{14}H_{12}BrN_2O$ (MH^+), 303.0128, found 303.0142.

5-[(3-Methylphenyl)methoxy]-1H-indazole (4i)

Yield: 5.6%; mp 144–147 °C; ^{1}H NMR (600 MHz, DMSO-d_6) δ 12.92 (s, 1H), 7.94 (s, 1H), 7.46 (d, $J = 8.9$ Hz, 1H), 7.31–7.28 (m, 2H), 7.28 – 7.24 (m, 2H), 7.14 (d, $J = 7.1$ Hz, 1H), 7.08 (dd, $J = 8.9$, 2.3 Hz, 1H), 5.07 (s, 2H), 2.33 (s, 3H); ^{13}C NMR (150 MHz, DMSO-d_6) δ 153.30, 138.00, 137.69, 136.26, 133.30, 128.82, 128.76, 128.68, 125.22, 123.52, 118.81, 111.51, 101.76, 70.17, 21.47; APCI-HRMS m/z: calculated for $C_{15}H_{15}N_2O$ (MH^+), 239.1179, found 239.1181.

6-(Benzyloxy)-1H-indazole (5a)

Yield: 18.4%; mp 161–163 °C; ^{1}H NMR (600 MHz, DMSO-d_6) δ 12.78 (s, 1H), 7.93 (s, 1H), 7.63 (d, $J = 8.8$ Hz, 1H), 7.52–7.46 (m, 2H), 7.41 (t, $J = 7.9$ Hz, 2H), 7.34 (t, $J = 7.6$ Hz, 1H), 7.05 – 6.99 (m, 1H), 6.83 (dd, $J = 8.7$, 2.1 Hz, 1H), 5.18 (s, 2H); ^{13}C NMR (150 MHz, DMSO-d_6) δ 158.05, 141.45, 137.53, 133.82, 128.89, 128.24, 128.05, 121.72, 118.23, 113.12, 92.81, 69.94; APCI-HRMS m/z: calculated for $C_{14}H_{13}N_2O$ (MH^+), 225.1022, found 225.1032.

6-[(4-Fluorophenyl)methoxy]-1H-indazole (5b)

Yield: 13.4%; mp 132–134 °C; ^{1}H NMR (600 MHz, DMSO-d_6) δ 12.79 (s, 1H), 7.94 (s, 1H), 7.63 (d, $J = 8.7$ Hz, 1H), 7.57 – 7.50 (m, 2H), 7.23 (t, $J = 8.9$ Hz, 2H), 7.04 – 6.99 (m, 1H), 6.82 (dd, $J = 8.8$, 2.1 Hz, 1H), 5.16 (s, 2H); ^{13}C NMR (150 MHz, DMSO-d_6) δ 163.03, 161.41, 157.94, 141.43, 133.83, 133.75, 133.73, 130.33, 130.27, 121.74, 118.27, 115.76, 115.62, 113.09, 92.84, 69.23; APCI-HRMS m/z: calculated for $C_{14}H_{12}FN_2O$ (MH^+), 243.0928, found 243.0919.

6-[(4-Chlorophenyl)methoxy]-1H-indazole (5c)

Yield: 11.9%; mp 142.5–148 °C; ^{1}H NMR (600 MHz, DMSO-d_6) δ 12.79 (s, 1H), 7.94 (s, 1H), 7.64 (d, $J = 8.7$ Hz, 1H), 7.54 – 7.49 (m, 2H), 7.48 – 7.44 (m, 2H), 7.03 – 6.98 (m, 1H), 6.83 (dd, $J = 8.8$, 2.2 Hz, 1H), 5.18 (s, 2H); ^{13}C NMR (150 MHz, DMSO-d_6) δ 157.85, 141.41, 136.60, 133.83, 132.84, 129.84, 128.89, 121.77, 118.31, 113.06, 92.90, 69.11; APCI-HRMS m/z: calculated for $C_{14}H_{12}ClN_2O$ (MH^+), 259.0633, found 259.0643.

6-[(4-Bromophenyl)methoxy]-1H-indazole (5d)

Yield: 10.6%; mp 167–169 °C; ^{1}H NMR (600 MHz, DMSO-d_6) δ 12.83 (s, 1H), 7.94 (s, 1H), 7.64 (d, $J = 8.8$ Hz, 1H), 7.60 (d, $J = 8.3$ Hz, 2H), 7.45 (d, $J = 8.4$ Hz, 2H), 7.03 – 6.96 (m, 1H), 6.82 (dd, $J = 8.7$, 2.1 Hz, 1H), 5.16 (s, 2H); ^{13}C NMR (150 MHz, DMSO-d_6) δ 157.80, 141.36, 137.01, 133.84, 131.83, 130.18, 121.79, 121.35, 118.26, 113.07, 92.79, 69.06; APCI-HRMS m/z: calculated for $C_{14}H_{12}BrN_2O$ (MH^+), 303.0128, found 303.0115.

6-[(4-Methylphenyl)methoxy]-1H-indazole (5e)

Yield: 10.2%; mp 147–149 °C; ^{1}H NMR (600 MHz, DMSO-d_6) δ 12.83 (s, 1H), 7.94 (s, 1H), 7.62 (d, $J = 8.8$ Hz, 1H), 7.37 (d, $J = 7.9$ Hz, 2H), 7.21 (d, $J = 7.8$ Hz, 2H), 7.02 – 6.97 (m, 1H), 6.80 (dd, $J = 8.7$, 2.1 Hz, 1H), 5.12 (s, 2H), 2.31 (s, 3H); ^{13}C NMR

(150 MHz, DMSO-d_6) δ 158.03, 141.41, 137.50, 134.43, 133.81, 129.45, 128.19, 121.71, 118.12, 113.19, 92.65, 69.75, 21.24; APCI-HRMS m/z: calculated for $C_{15}H_{15}N_2O$ (MH^+), 239.1179, found 239.1169.

6-[(3-Bromophenyl)methoxy]-1H-indazole (5f)

Yield: 12.4%; mp 146.7–149 °C; ^{1}H NMR (600 MHz, DMSO-d_6) δ 12.82 (s, 1H), 7.94 (s, 1H), 7.71 – 7.68 (m, 1H), 7.64 (d, $J = 8.8$ Hz, 1H), 7.57 – 7.47 (m, 2H), 7.38 (t, $J = 7.8$ Hz, 1H), 7.03 – 6.98 (m, 1H), 6.84 (dd, $J = 8.7$, 2.1 Hz, 1H), 5.20 (s, 2H); ^{13}C NMR (150 MHz, DMSO-d_6) δ 157.77, 141.37, 140.40, 133.84, 131.13, 131.08, 130.56, 126.94, 122.16, 121.82, 118.31, 113.06, 92.83, 68.91; APCI-HRMS m/z: calculated for $C_{14}H_{12}BrN_2O$ (MH^+), 303.0128, found 303.0129.

MAO activity measurements

The activities of MAO-A and MAO-B were measured by following the procedure as reported in literature [47, 50]. For this purpose, kynuramine was used as a mixed substrate and commercially available recombinant human MAO-A and MAO-B served as enzyme sources. Kynuramine is oxidized by MAO to produce 4-hydroxyquinoline as final product. Fluorescence spectrophotometry was used to measure 4-hydroxyquinoline following the alkalinization of the reactions at the end-point.

DAAO activity measurements

To measure the activity of DAAO, a previously reported protocol was followed [37, 48, 51]. D-Serine served as the substrate and porcine kidney DAAO was used as enzyme source. H_2O_2, a by-product of the catalytic cycle of DAAO, was measured in a peroxidase-coupled assay system using the reagent, Amplex red. In the presence of H_2O_2, horseradish peroxidase catalyzes the oxidation of Amplex red to yield the fluorescent compound, resorufin. Fluorescence spectrophotometry was used to continuously measure resorufin formation.

To investigate the possibility that a test inhibitor may suppress the fluorescence signal produced in the peroxidase-coupled assay system, the test inhibitor at 1, 10 and 100 μM was incubated with horse radish peroxidase, Amplex red and hydrogen peroxide and the fluorescence intensities were measured. These data were compared to control experiments conducted in the absence of inhibitor. The protocol for this experiment has been reported [51].

Molecular docking

Molecular docking was performed according to the protocol previously described [47]. The Discovery Studio 3.1 suite was used and X-ray crystal structures of MAO-A (PDB code: 2Z5X) and MAO-B (PDB code: 2V5Z) bound to harmine and safinamide, respectively, were selected as the protein models [42, 46]. Illustrations were created with the PyMOL molecular graphics system [52].

Acknowledgements This work was financially supported by the National Research Foundation of South Africa [Grant specific unique reference numbers (UID) 137997 and 132168]. The Grantholders acknowledge that opinions, findings and conclusions or recommendations expressed in any publication generated by the NRF supported research are that of the authors, and that the NRF accepts no liability whatsoever in this regard.

Funding Open access funding provided by North-West University.

Compliance with ethical standards

Conflict of Interest The authors declare no competing interests.

Publisher's note Springer Nature remains neutral with regard to jurisdictional claims in published maps and institutional affiliations.

Abbreviations

DAAO	D-amino acid oxidase
DMF	N,N-dimethylformamide
DMSO	dimethyl sulfoxide
HRMS	high resolution mass spectrometry
MAO	monoamine oxidase
NMDA	N-methyl-D-aspartate
NMR	nuclear magnetic resonance
nNOS	neuronal nitric oxide synthase
SD	standard deviation
TLC	thin layer chromatography

References

1. Barone P. Neurotransmission in Parkinson's disease: beyond dopamine. Eur J Neurol. 2010;17:364–76. https://doi.org/10.1111/j.1468-1331.2009.02900.x
2. Millan MJ. N-Methyl-D-aspartate receptors as a target for improved antipsychotic agents: novel insights and clinical perspectives. Psychopharmacology (Berl). 2005;179:30–53. https://doi.org/10.1007/s00213-005-2199-1

3. Werner FM, Covenas R. Classical neurotransmitters and neuropeptides involved in major depression: a review. Int J Neurosci. 2010;120:455–70. https://doi.org/10.3109/00207454.2010.483651
4. Lane HY, Lin CH, Green MF, Hellemann G, Huang CC, Chen PW, et al. Add-on treatment of benzoate for schizophrenia: a randomized, double-blind, placebo-controlled trial of D-amino acid oxidase inhibitor. JAMA Psychiatry. 2013;70:1267–75. https://doi.org/10.1001/jamapsychiatry.2013.2159
5. Youdim MB, Edmondson D, Tipton KF. The therapeutic potential of monoamine oxidase inhibitors. Nat Rev Neurosci. 2006;7:295–309. https://doi.org/10.1038/nrn1883
6. Fowler JS, MacGregor RR, Wolf AP, Arnett CD, Dewey SL, Schlyer D, et al. Mapping human brain monoamine oxidase A and B with 11C-labeled suicide inactivators and PET. Science. 1987;235:481–5. https://doi.org/10.1126/science.3099392
7. Rodriguez MJ, Saura J, Billett EE, Finch CC, Mahy N. Cellular localization of monoamine oxidase A and B in human tissues outside of the central nervous system. Cell Tissue Res. 2001;304:215–20. https://doi.org/10.1007/s004410100361
8. Youdim MB, Bakhle YS. Monoamine oxidase: isoforms and inhibitors in Parkinson's disease and depressive illness. Br J Pharmacol. 2006;147:S287–96. https://doi.org/10.1038/sj.bjp.0706464
9. Bach AW, Lan NC, Johnson DL, Abell CW, Bembenek ME, Kwan SW, et al. cDNA cloning of human liver monoamine oxidase A and B: molecular basis of differences in enzymatic properties. Proc Natl Acad Sci USA. 1988;85:4934–8. https://doi.org/10.1073/pnas.85.13.4934
10. Shih JC. Monoamine oxidase isoenzymes: genes, functions and targets for behavior and cancer therapy. J Neural Transm (Vienna). 2018;125:1553–66. https://doi.org/10.1007/s00702-018-1927-8
11. Edmondson DE. Hydrogen peroxide produced by mitochondrial monoamine oxidase catalysis: biological implications. Curr Pharm Des. 2014;20:155–60. https://doi.org/10.2174/13816128113190990406
12. Bortolato M, Chen K, Shih JC. Monoamine oxidase inactivation: from pathophysiology to therapeutics. Adv Drug Deliv Rev. 2008;60:1527–33. https://doi.org/10.1016/j.addr.2008.06.002
13. Meyer JH, Ginovart N, Boovariwala A, Sagrati S, Hussey D, Garcia A, et al. Elevated monoamine oxidase a levels in the brain: an explanation for the monoamine imbalance of major depression. Arch Gen Psychiatry. 2006;63:1209–16. https://doi.org/10.1001/archpsyc.63.11.1209
14. Shulman KI, Herrmann N, Walker SE. Current place of monoamine oxidase inhibitors in the treatment of depression. CNS Drugs. 2013;27:789–97. https://doi.org/10.1007/s40263-013-0097-3
15. Suchting R, Tirumalajaru V, Gareeb R, Bockmann T, de Dios C, Aickareth J, et al. Revisiting monoamine oxidase inhibitors for the treatment of depressive disorders: A systematic review and network meta-analysis. J Affect Disord. 2021;282:1153–60. https://doi.org/10.1016/j.jad.2021.01.021
16. Fowler CJ, Wiberg A, Oreland L, Marcusson J, Winblad B. The effect of age on the activity and molecular properties of human brain monoamine oxidase. J Neural Transm. 1980;49:1–20. https://doi.org/10.1007/BF01249185
17. Tong J, Meyer JH, Furukawa Y, Boileau I, Chang LJ, Wilson AA, et al. Distribution of monoamine oxidase proteins in human brain: implications for brain imaging studies. J Cereb Blood Flow Metab. 2013;33:863–71. https://doi.org/10.1038/jcbfm.2013.19
18. Berry MD, Scarr E, Zhu MY, Paterson IA, Juorio AV. The effects of administration of monoamine oxidase-B inhibitors on rat striatal neurone responses to dopamine. Br J Pharmacol. 1994;113:1159–66. https://doi.org/10.1111/j.1476-5381.1994.tb17119.x
19. Robakis D, Fahn S. Defining the role of the monoamine oxidase-B inhibitors for Parkinson's disease. CNS Drugs. 2015;29:433–41. https://doi.org/10.1007/s40263-015-0249-8
20. Pizzinat N, Copin N, Vindis C, Parini A, Cambon C. Reactive oxygen species production by monoamine oxidases in intact cells. Naunyn Schmiedebergs Arch Pharmacol. 1999;359:428–31. https://doi.org/10.1007/pl00005371
21. Cohen G. Monoamine oxidase and oxidative stress at dopaminergic synapses. J Neural Transm Suppl. 1990;32:229–38. https://doi.org/10.1007/978-3-7091-9113-2_33
22. Fernandez HH, Chen JJ. Monoamine oxidase-B inhibition in the treatment of Parkinson's disease. Pharmacotherapy. 2007;27:174S–85S. https://doi.org/10.1592/phco.27.12part2.174S
23. Finberg JP, Rabey JM. Inhibitors of MAO-A and MAO-B in psychiatry and neurology. Front Pharmacol. 2016;7:340. https://doi.org/10.3389/fphar.2016.00340
24. Kumar B, Gupta VP, Kumar V. A perspective on monoamine oxidase enzyme as drug target: challenges and opportunities. Curr Drug Targets. 2017;18:87–97. https://doi.org/10.2174/1389450117666151209123402
25. Stowe R, Ives N, Clarke CE, Handley K, Furmston A, Deane K, et al. Meta-analysis of the comparative efficacy and safety of adjuvant treatment to levodopa in later Parkinson's disease. Mov Disord. 2011;26:587–98. https://doi.org/10.1002/mds.23517
26. Tan YY, Jenner P, Chen SD. Monoamine oxidase-B inhibitors for the treatment of Parkinson's disease: past, present, and future. J Parkinsons Dis. 2022;12:477–93. https://doi.org/10.3233/JPD-212976
27. Katane M, Osaka N, Matsuda S, Maeda K, Kawata T, Saitoh Y, et al. Identification of novel D-amino acid oxidase inhibitors by in silico screening and their functional characterization in vitro. J Med Chem. 2013;56:1894–907. https://doi.org/10.1021/jm3017865
28. Pollegioni L, Sacchi S, Murtas G. Human D-amino acid oxidase: structure, function, and regulation. Front Mol Biosci. 2018;5:107. https://doi.org/10.3389/fmolb.2018.00107
29. Mothet JP, Parent AT, Wolosker H, Brady RO Jr, Linden DJ, Ferris CD, et al. D-Serine is an endogenous ligand for the glycine site of the N-methyl-D-aspartate receptor. Proc Natl Acad Sci USA. 2000;97:4926–31. https://doi.org/10.1073/pnas.97.9.4926
30. Wolosker H. NMDA receptor regulation by D-serine: new findings and perspectives. Mol Neurobiol. 2007;36:152–64. https://doi.org/10.1007/s12035-007-0038-6
31. Duplantier AJ, Becker SL, Bohanon MJ, Borzilleri KA, Chrunyk BA, Downs JT, et al. Discovery, SAR, and pharmacokinetics of a novel 3-hydroxyquinolin-2(1H)-one series of potent D-amino acid oxidase (DAAO) inhibitors. J Med Chem. 2009;52:3576–85. https://doi.org/10.1021/jm900128w
32. Heresco-Levy U, Javitt DC, Ebstein R, Vass A, Lichtenberg P, Bar G, et al. D-Serine efficacy as add-on pharmacotherapy to risperidone and olanzapine for treatment-refractory schizophrenia. Biol Psychiatry. 2005;57:577–85. https://doi.org/10.1016/j.biopsych.2004.12.037
33. Kantrowitz JT, Malhotra AK, Cornblatt B, Silipo G, Balla A, Suckow RF, et al. High dose D-serine in the treatment of schizophrenia. Schizophr Res. 2010;121:125–30. https://doi.org/10.1016/j.schres.2010.05.012
34. Maekawa M, Okamura T, Kasai N, Hori Y, Summer KH, Konno R. D-amino-acid oxidase is involved in D-serine-induced nephrotoxicity. Chem Res Toxicol. 2005;18:1678–82. https://doi.org/10.1021/tx0500326
35. Nishikawa T. Analysis of free D-serine in mammals and its biological relevance. J Chromatogr B Analyt Technol Biomed Life Sci. 2011;879:3169–83. https://doi.org/10.1016/j.jchromb.2011.08.030
36. Ferraris D, Duvall B, Ko YS, Thomas AG, Rojas C, Majer P, et al. Synthesis and biological evaluation of D-amino acid oxidase

inhibitors. J Med Chem. 2008;51:3357–9. https://doi.org/10.1021/jm800200u
37. Hondo T, Warizaya M, Niimi T, Namatame I, Yamaguchi T, Nakanishi K, et al. 4-Hydroxypyridazin-3(2H)-one derivatives as novel D-amino acid oxidase inhibitors. J Med Chem. 2013;56:3582–92. https://doi.org/10.1021/jm400095b
38. Sparey T, Abeywickrema P, Almond S, Brandon N, Byrne N, Campbell A, et al. The discovery of fused pyrrole carboxylic acids as novel, potent D-amino acid oxidase (DAO) inhibitors. Bioorg Med Chem Lett. 2008;18:3386–91. https://doi.org/10.1016/j.bmcl.2008.04.020
39. Castagnoli K, Palmer S, Anderson A, Bueters T, Castagnoli N Jr. The neuronal nitric oxide synthase inhibitor 7-nitroindazole also inhibits the monoamine oxidase-B-catalyzed oxidation of 1-methyl-4-phenyl-1,2,3,6-tetrahydropyridine. Chem Res Toxicol. 1997;10:364–8. https://doi.org/10.1021/tx970001d
40. Di Monte DA, Royland JE, Anderson A, Castagnoli K, Castagnoli N Jr, Langston JW. Inhibition of monoamine oxidase contributes to the protective effect of 7-nitroindazole against MPTP neurotoxicity. J Neurochem. 1997;69:1771–3. https://doi.org/10.1046/j.1471-4159.1997.69041771.x
41. Binda C, Li M, Hubalek F, Restelli N, Edmondson DE, Mattevi A. Insights into the mode of inhibition of human mitochondrial monoamine oxidase B from high-resolution crystal structures. Proc Natl Acad Sci USA. 2003;100:9750–5. https://doi.org/10.1073/pnas.1633804100
42. Binda C, Wang J, Pisani L, Caccia C, Carotti A, Salvati P, et al. Structures of human monoamine oxidase B complexes with selective noncovalent inhibitors: safinamide and coumarin analogs. J Med Chem. 2007;50:5848–52. https://doi.org/10.1021/jm070677y
43. Hubalek F, Binda C, Khalil A, Li M, Mattevi A, Castagnoli N, et al. Demonstration of isoleucine 199 as a structural determinant for the selective inhibition of human monoamine oxidase B by specific reversible inhibitors. J Biol Chem. 2005;280:15761–6. https://doi.org/10.1074/jbc.M500949200
44. Manley-King CI, Bergh JJ, Petzer JP. Inhibition of monoamine oxidase by selected C5- and C6-substituted isatin analogues. Bioorg Med Chem. 2011;19:261–74. https://doi.org/10.1016/j.bmc.2010.11.028
45. Van der Walt EM, Milczek EM, Malan SF, Edmondson DE, Castagnoli N Jr, Bergh JJ, et al. Inhibition of monoamine oxidase by (E)-styrylisatin analogues. Bioorg Med Chem Lett. 2009;19:2509–13. https://doi.org/10.1016/j.bmcl.2009.03.030
46. Son SY, Ma J, Kondou Y, Yoshimura M, Yamashita E, Tsukihara T. Structure of human monoamine oxidase A at 2.2-A resolution: the control of opening the entry for substrates/inhibitors. Proc Natl Acad Sci USA. 2008;105:5739–44. https://doi.org/10.1073/pnas.0710626105
47. Mostert S, Petzer A, Petzer JP. Indanones as high-potency reversible inhibitors of monoamine oxidase. ChemMedChem. 2015;10:862–73. https://doi.org/10.1002/cmdc.201500059
48. Zhou M, Panchuk-Voloshina N. A one-step fluorometric method for the continuous measurement of monoamine oxidase activity. Anal Biochem. 1997;253:169–74. https://doi.org/10.1006/abio.1997.2392
49. Molla G. Competitive inhibitors unveil structure/function relationships in human D-amino acid oxidase. Front Mol Biosci. 2017;4:80. https://doi.org/10.3389/fmolb.2017.00080
50. Weissbach H, Smith TE, Daly JW, Witkop B, Udenfriend S. A rapid spectrophotometric assay of mono-amine oxidase based on the rate of disappearance of kynuramine. J Biol Chem. 1960;235:1160–3
51. Bester E, Petzer A, Petzer JP. Coumarin derivatives as inhibitors of d-amino acid oxidase and monoamine oxidase. Bioorg Chem. 2022;123:105791. https://doi.org/10.1016/j.bioorg.2022.105791
52. DeLano WL. The PyMOL molecular graphics system. San Carlos, USA: DeLano Scientific; 2002